
Differentiable Optimization-based Control Policy with Convergence Analysis

Yuexin Bian¹ Jie Feng¹ Yuanyuan Shi¹

Abstract

Real-world system control requires both high-performing and interpretable controllers. Model-based control policies have gained popularity by using historical data to learn system costs and dynamics before implementation. However, this two-phase approach prevents these policies from achieving optimal control as the metrics that we train these models (e.g., mean squared errors) often differ from the actual control system cost. In this paper, we present DiffOP, a Differentiable Optimization-based Policy for optimal control. In the proposed framework, control actions are derived by solving an optimization, where the control cost function and system’s dynamics can be parameterized as neural networks. Our key technical innovation lies in developing a hybrid optimization algorithm that combines policy gradients with implicit differentiation through the optimization layer, enabling end-to-end training with the actual cost feedback. Under standard regularity conditions, we prove DiffOP converges to stationary points at a rate of $O(1/K)$. Empirically, DiffOP achieves state-of-the-art performance in both nonlinear control tasks and real-world building control.

1. Introduction

Operating and controlling complex systems in an effective manner is of critical importance to society. Real-world physical systems, such as power grids (Machowski et al., 2020), commercial and industrial infrastructures (Chen et al., 2019b), transportation networks (Negenborn et al., 2008), and robotic systems (Spong et al., 2020), require control policies that are not only high-performing but also interpretable to ensure efficiency, reliability, and safety. To this end, optimization-based policies such as model predictive control have been explored with known (Morari & Lee, 1999; Grüne et al., 2017) or learned system dynamics (Chen et al., 2019b; Jin et al., 2020), aiming to optimize performance, incorporate constraints, and provide interpretability of the decision-making process.

Optimization-based policies formulate the control problem

as a mathematical optimization problem, where the objective is to minimize the system cost, subjective to the system dynamics model and state/action constraints. In this area, previous works (Chen et al., 2019b; Jin et al., 2020; Amos et al., 2018; Killian & Kozek, 2016) have primarily focused on learning cost and dynamic models by minimizing prediction errors on the historical data (e.g., mean squared errors). However, these approaches often overlook the ultimate objective of control systems: minimizing actual control costs. This divergence in learning process can lead to a model that, despite having a high accuracy in predicting past data, struggles to perform optimally when it comes to guiding control decisions and minimizing real-world operational costs (Donti et al., 2017; Jain et al., 2021; Gros & Zanon, 2021; Elmachtoub & Grigas, 2022; Mandi et al., 2024).

To enhance closed-loop performance in accordance with control objectives, researchers have explored combining optimization-based policies with model-free Reinforcement Learning (RL) techniques (Chen et al., 2019a; Jain et al., 2021; Gros & Zanon, 2019; 2021; Drgoňa et al., 2024; Wan et al., 2024). However, integrating neural networks into the optimization policy is computationally expensive due to the need for deriving implicit gradients (Xu et al., 2024). Furthermore, the absence of nonasymptotic convergence analysis represents a significant gap in the literature.

In response to these challenges, we present DiffOP, an innovative optimal control framework with a **Differentiable Optimization-based Policy**. This approach considers an optimization-based control policy (based on model predictive control), allowing for the representation of both the cost function and dynamics through either physics-based models or neural networks, and optimize the policy parameters via reinforcement learning with actual cost feedback. Our key contributions can be summarized as follows,

(1) DiffOP framework: We propose DiffOP, an optimal control framework to learn the optimization-based control policy from the actual cost feedback when interacting with the system. A key technical contribution of this work is the introduction of a joint learning approach that leverages implicit differentiation (Xu et al., 2024; Jin et al., 2020) and policy gradients (Sutton & Barto, 2018) to simultaneously learn the cost and dynamics models. This method enables the computation of analytical policy gradients for

the optimization-based policy within the model-free RL context. Experiments across various system control tasks demonstrate DiffOP’s superior performance compared to state-of-the-art baselines, including model-based optimization methods and model-free RL methods.

(2) Theoretical Guarantee: To provide the theoretical guarantee for DiffOP, we adopt policy gradient algorithm as the policy optimizer and investigate the convergence of DiffOP. To the best of our knowledge, this study is the first to provide a theoretical analysis of convergence rates and sample complexity for an optimization-based policy in the reinforcement learning setting. In particular, we show that the algorithm requires at most the total number of $K = \mathcal{O}(\epsilon^{-1})$ of iterations to achieve an ϵ -accurate stationary point.

2. Related Work

Differentiable Optimization for Optimal Control. Recent research has demonstrated the feasibility of differentiating through optimization problems using implicit differentiation of the optimality conditions (Amos & Kolter, 2017; Agrawal et al., 2019; Jin et al., 2020; Xu et al., 2024) or standard unrolling (Pineda et al., 2022; Okada et al., 2017). In the context of optimal control, optimization has been employed as a control policy, e.g., in model predictive control (Morari & Lee, 1999; Grüne et al., 2017; Chen et al., 2019a;b; Wan et al., 2024) and Pontryagin’s maximum principle (Jin et al., 2020). Several works are relevant to our approach: (Jin et al., 2020) proposed an optimization policy that jointly learns cost and dynamics functions via pontryagin differentiable programming, while (Chen et al., 2019b) developed a convex model predictive control (MPC) policy using input convex neural networks (Amos et al., 2017) to address the trade-off between modeling accuracy and control tractability. However, these approaches either require expert demonstrations or large historical datasets, and their supervised learning methods may lead to misalignment between the learned model and the actual control objectives.

(Gros & Zanon, 2021) and (Chen et al., 2019a) both explored reinforcement learning (RL) with stochastic MPC policies, while the former through cost objective perturbation and the latter using Gaussian noise. Both methods adopt a model-free RL framework to align the model learning and control performance. However, these approaches are constrained by their focus on linear dynamics and quadratic cost functions, and their frameworks lack theoretical guarantees. Our work advances the field by learning optimization-based policies with neural network-parameterized cost and dynamic models, that jointly optimized through model-free RL algorithm with convergence analysis.

Model-based Reinforcement Learning. Model-based RL is typically more sample efficient than model-free RL due

to learning dynamics through supervised learning (Wan et al., 2024), though it faces an “objective mismatch” problem (Lambert et al., 2020). Recent approaches address the objective mismatch problem by jointly optimizing the control policy and dynamics models (Eysenbach et al., 2022; Vemula et al., 2023). Our method differs from model-based RL by enabling end-to-end training of both cost and dynamics models through a hybrid optimization approach that combines policy gradients with implicit differentiation using actual cost feedback. A concurrent work (Wan et al., 2024) also explores implicit optimization for policy representation but differs in two key aspects: i) it relies on Q-function learning for policy optimization, whereas we derive the analytical policy gradients through implicit differentiation; ii) we provide the theoretical convergence and sample complexity guarantees for the proposed algorithm.

Convergence Analysis of Policy Gradient Algorithm.

The convergence rates of policy gradient (PG) algorithms have been well established in (Sutton et al., 1999; Scherrer, 2014; Papini et al., 2018; Fazel et al., 2018; Agarwal et al., 2020). However, these approaches mostly consider explicit control policies such as linear policies and neural network policies. Recent research has expanded the scope of PG algorithms to more specialized settings, including softmax policies (Xu et al., 2021), time-invariant linear policies (Giegrich et al., 2024), and policies that integrate both feedback policy and predictive dynamics models (Hao et al., 2023). Our work advances the field by analyzing policies that emerge from optimization problems with learnable parameters in their objectives and constraints. To the best of our knowledge, we are the first to characterize the convergence properties of such implicit optimization-based policies within the policy gradient framework.

3. DiffOP: Optimal Control with a Differentiable Optimization-based Policy

In this work, we propose **DiffOP**, an optimal control framework with a Differentiable Optimization-based Policy that integrates both cost and dynamics model learning, as shown in Figure 1.

3.1. Differentiable Optimization-based Control Policy

The DiffOP policy is expressed in Equation (1), where H is the planning horizon, $x_{\text{init}} \in \mathbb{R}^n$ is the initial state. We denote $x_i \in \mathbb{R}^n, u_i \in \mathbb{R}^m$ as the system state and control action at the i -th planning step, respectively. $c(x_i, u_i; \theta_c), c_H(x_H; \theta_H)$ model the instantaneous and terminal costs with learnable parameter θ_c and θ_H , $f(x_i, u_i; \theta_f)$ models system dynamics with learnable parameters θ_f , and $g(\cdot)$ represents the state and control con-

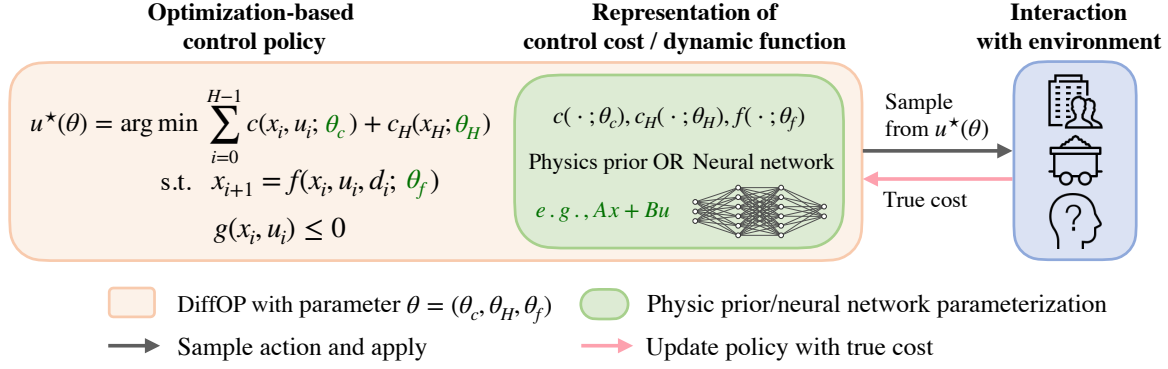


Figure 1. DiffOP: an optimal control framework with a differentiable optimization-based policy. The cost model and dynamic model within the optimization can be represented by neural networks or equations with unknown parameters. The framework leverages policy gradients combined with implicit differentiation to jointly optimize the cost and dynamics models using actual cost feedback when interacting with the unknown environment.

straints, which are known to the control agent.

$$\begin{aligned}
 u_{0:H-1}^*(x_{\text{init}}; \theta) = \arg \min_u \sum_{i=0}^{H-1} c(x_i, u_i; \theta_c) + c_H(x_H; \theta_H) \\
 \text{subject to } x_0 = x_{\text{init}}, \\
 x_{i+1} = f(x_i, u_i; \theta_f), \\
 g(x_i, u_i) \leq 0.
 \end{aligned} \tag{1}$$

In summary, the optimization policy (1) is represented by some parametric representation (e.g. neural networks) of the cost and dynamics functions with parameters $\theta = (\theta_c, \theta_H, \theta_f) \in \mathbb{R}^d$.

For a given system state x , the action can be determined by solving the optimization policy (1),

$$\pi_\theta(x) = u_0^*(x; \theta), \tag{2}$$

where u_0^* is the first element of the solution sequence $u_0^*, u_1^*, \dots, u_{H-1}^*$ obtained from (1). The proposed optimization control policy offers interpretability, which allows system operators and engineers to understand how the control decisions are determined based on the system costs and the dynamics - an advantage that neural network control policies may lack. Further, it can conveniently incorporate constraints on the state and action, to ensure safety and other real-world operation requirements.

3.2. Optimal Control Problem Formulation

We are interested in optimizing the parameters in the DiffOP policy $\theta = (\theta_c, \theta_H, \theta_f) \in \mathbb{R}^d$, to minimize the overall control costs. The policy optimization problem is formulated

as follows,

$$\min_{\theta} C(\theta) := \mathbb{E} \left[\sum_{t=0}^T c(x_t, u_t; \phi_c) \right] \tag{3a}$$

$$\text{subject to } x_{t+1} = f(x_t, u_t; \phi_f), t = 0, \dots, T-1, \tag{3b}$$

$$u_t \sim \pi_\theta(x_t). \tag{3c}$$

Unknown system (3a)(3b): Equation (3a) describes the system cost model with ϕ_c and equation (3b) describes system dynamics parameterized by ϕ_f . We note that the ground truth parameters ϕ_c, ϕ_f are unknown.

Stochastic policy (3c): To facilitate exploration in finding the optimal policy, we introduce stochasticity by reparameterizing the policy as a Truncated Gaussian distribution in (3c):

$$u_t \sim \pi_\theta(x_t) = \mathcal{N}(u_t^*, \sigma^2 I, u_t^* \pm \beta \sigma^2 I), \tag{4}$$

where $u_t^* = \pi_\theta(x_t)$ represents the mean, defined in (2) by solving the optimization-based policy. The term $\sigma^2 I$ is the covariance matrix, with σ^2 being the variance and $I \in \mathbb{R}^{m \times m}$ denoting the identity matrix. The truncation range $u_t^* \pm \beta \sigma^2 I$ constrains the sampled actions within the specified bounds, where $\sigma > 0, \beta > 0$ are hyperparameters that control the exploration variance and truncation bounds, respectively.

We note that for the objective function in the optimal control problem (3), the expectation \mathbb{E} is taken with respect to the initial state distribution $x_0 \sim \mathcal{D}$, and the trajectory $(x_0, u_0, \dots, x_T, u_T)$ which is generated under the stochastic policy (3c). By choosing a Truncated Gaussian distribution over a traditional Gaussian distribution, we can bound the deviation of the sampled action from the optimal action. This bounded deviation contributes to establishing the

boundedness of the policy gradients, which provides good property for the convergence analysis of our algorithm.

Overall, (3c) involves solving an optimization problem, and the optimal control problem (3) is a stochastic bi-level optimization problem.

4. Proposed Algorithm

Our algorithm, DiffOP, is inspired by the classic policy gradient algorithm (Sutton & Barto, 2018; Papini et al., 2018), with differentiable optimization (Xu et al., 2024) for obtaining the gradient of the control action with respect to $\theta := \{\theta_c, \theta_H, \theta_f\}$ including the cost parameters θ_c, θ_H and dynamic model parameters θ_f . In the context of policy gradient, the algorithm works as follows. At each iteration k , we evaluate the policy performance $C(\theta^{(k)})$ with N trajectory sampled from the current policy $\theta^{(k)}$. The learner updates its policy parameters by taking a gradient step $\theta^{(k+1)} \leftarrow \theta^{(k)} - \eta \nabla_{\theta} C(\theta)$, where the gradient is computed as a combination of the policy gradients and gradients of the optimization problem at its solution. Let $\tau = (x_0, u_0, x_1, u_1, \dots, u_{T-1}, x_T)$ be the trajectory induced by the policy. The analytical policy gradient update rule would be the following:

Proposition 4.1 (Policy gradient update). *Consider the policy optimization with DiffOP policy in (3), the policy gradient takes the analytical form of:*

$$\nabla_{\theta} C(\theta) = \mathbb{E} \left[L(\tau) \left(\sum_{t=0}^T \frac{1}{\sigma^2} [\nabla_{\theta} u_t^*]^{\top} (u_t - u_t^*) \right) \right], \quad (5)$$

where u_t, u_t^* are the actual control action and correspond optimal solution derived by the policy at time t .

Proof. Proven in Appendix A. \square

In practice, one can use Monte Carlo sampling to evaluate the policy gradient with N trajectories:

$$\widehat{\nabla}_{\theta} C(\theta^{(k)}) = \frac{1}{N} \sum_{n=1}^N \left[L(\tau^{(n)}) \sum_{t=0}^T \frac{1}{\sigma^2} \nabla_{\theta} u_t^{*(n)\top} (u_t^{(n)} - u_t^{*(n)}) \right] \quad (6)$$

To evaluate policy gradient (5), $\nabla_{\theta} u_t^*$, the gradient of the optimal solution u^* w.r.t. θ is needed, which is given in the next Proposition.

Proposition 4.2 utilizes the first-order optimality conditions and the implicit function theorem to establish the relationship between the solution of the optimization-based policy and the policy parameters. We begin by defining x_i^*, u_i^* as the optimal state and action obtained by solving the optimization policy (1), where $i = 0, \dots, H - 1$

1 denotes the i -th planning step. We further define $\zeta^* = (x_0^*, u_0^*, x_1^*, u_1^*, \dots, u_{H-1}^*, x_H^*)$ as the optimal solution trajectory over the horizon H . We stack all constraints into a single vector-valued constraint $\kappa := (\kappa_{-1}, \kappa_0, \kappa_1, \dots, \kappa_H) \in \mathbb{R}^{n_{\kappa}}$, $n_{\kappa} = (H+1)n + q$. Specifically, $\kappa_{-1} = x_0^*$ is the input to the policy, and

$$\kappa_i = \begin{cases} (\tilde{g}(x_i^*, u_i^*), x_{i+1}^* - f(x_i^*, u_i^*; \theta_f)), & i = 0, \dots, H-1, \\ \tilde{g}(x_H^*), & i = H, \end{cases} \quad (7)$$

where $\tilde{g}(x_i^*, u_i^*)$ are the subset of active inequality constraints at i -th planning step, and q is the total number of active inequality constraints. The optimization problem in (1) can be solved using general-purpose solvers (Gill et al., 2005; Diamond & Boyd, 2016) to determine both the optimal solution ζ^* and its associated active constraints κ .

Proposition 4.2 (Gradient of the optimization-based policy). *Suppose u^* is the solution of the optimization-based policy (1) and denote ζ^* as the resulting trajectory. Assume $c(\cdot), c_H(\cdot), f(\cdot), g(\cdot)$ are twice differentiable in a neighborhood of (θ, ζ^*) . Let*

$$\begin{aligned} A &= \nabla_{\zeta} \kappa(\zeta^*; \theta), \\ B &= \nabla_{\theta \zeta}^2 J(\zeta^*; \theta) - \sum_{i=-1}^H \sum_{j=1}^{|\kappa_i|} \lambda_{i,j} \nabla_{\theta \zeta}^2 [\kappa_i(\zeta^*; \theta)]_j, \\ C &= \nabla_{\theta} \kappa(\zeta^*; \theta), \\ D &= \nabla_{\zeta \zeta}^2 J(\zeta^*; \theta) - \sum_{i=-1}^H \sum_{j=1}^{|\kappa_i|} \lambda_{i,j} \nabla_{\zeta \zeta}^2 [\kappa_i(\zeta^*; \theta)]_j, \end{aligned}$$

If $\text{rank}(A) = n_{\kappa}$ and D is non-singular, then the gradient $\nabla_{\theta} u_0^*$ takes the following form,

$$\nabla_{\theta} u_0^* = [\nabla_{\theta} \zeta^*]_{n:n+m}, \quad (8)$$

with

$$\nabla_{\theta} \zeta^* = D^{-1} A^{\top} (A D^{-1} A^{\top})^{-1} (A D^{-1} B - C) - D^{-1} B,$$

where n, m are the state and action dimensions, and the Lagrange multiplier $\lambda \in \mathbb{R}^{n_{\kappa}}$ satisfies $\lambda^{\top} A = \nabla_{\zeta} J(\zeta^*; \theta)$.

We note that $\lambda_{i,j}$ is the dual variable corresponding to the j -th element of $\kappa_i(\zeta^*; \theta)$. Proposition 4.2 is a direct application of the constrained optimization differentiation (Xu et al., 2024; Gould et al., 2021) and its proof is included in the Appendix B for completeness.

Algorithm 1 presents DiffOP in its simplest form. At each iteration k , we estimate the policy gradient in (5) with N sampled trajectories, where the gradient of the optimization-based control policy is given in (8). It is worth noting that although we employ the REINFORCE algorithm (Sutton & Barto, 2018; Papini et al., 2018) to estimate the policy

Algorithm 1 Policy Optimization with Differentiable Optimization-based Policy (DiffOP)

Input: $\theta^{(0)} = (\theta_c^{(0)}, \theta_H^{(0)}, \theta_f^{(0)})$, learning rate η
for $k = 0, 1, \dots, K - 1$ **do**
 for $n = 1, \dots, N$ **do**
 Determine the action as in eq (1)(4), $\forall t$
 Collect the trajectory data $(x_t^{(n)}, u_t^{(n)}, u_t^{\star(n)})$, $\forall t$
 Calculate the gradient $\nabla_{\theta} u_t^{\star(n)}$, $\forall t$ as in eq (8)
 end for
 Estimate policy gradient $\hat{\nabla}_{\theta} C(\theta^{(k)})$ as in eq (6) with N trajectory data
 Update policy $\theta^{(k+1)} \leftarrow \theta^{(k)} - \eta \hat{\nabla}_{\theta} C(\theta^{(k)})$
end for

gradients, there are several techniques available to reduce the variance of the gradient estimator (Zhao et al., 2011; Grathwohl et al., 2017) which could be incorporated into the framework flexibly.

5. Non-Asymptotic Convergence Analysis

We now present our main theoretical result, which states the convergence of learning optimization-based control policy with policy gradients. For the theoretical analysis, we focus on the unconstrained optimization-based policy, i.e., (1) without state and action constraints.

For a given initial state $x_0 = x_{\text{init}}$ and control sequence $u = [u_0, \dots, u_{H-1}] \in \mathbb{R}^{mH}$ derived from the optimization-based policy with parameter θ , the unrolled cost function is defined as,

$$J(x_{\text{init}}, u, \theta) = \sum_{i=0}^{H-1} c(x_i, u_i; \theta_c) + c(x_H; \theta_H), \quad (9)$$

with $x_0 = x_{\text{init}}, x_{i+1} = f(x_i, u_i; \theta_f)$. Before stating our results, we discuss the technical assumptions and their implications. The first assumption is about the characterization of the optimization landscape.

Assumption 5.1. The function $J(x_{\text{init}}, u, \theta)$ is μ -strongly convex with respect to u .

The strong convexity of the objective function $J(x_{\text{init}}, u, \theta)$ guarantees both uniqueness of the optimal solution and injectivity of the policy mapping, ensuring stable convergence properties and well-defined state-input relationships in the control system. Further, let $z = (x_{\text{init}}, u, \theta) \in \mathbb{R}^{n_z}$, $z' = (x'_{\text{init}}, u', \theta') \in \mathbb{R}^{n_z}$ and $\|\cdot\|$ be the 2-norm of a vector and Frobenius norm of a matrix. The following assumption concerns the Lipschitz properties of the function $J(z)$.

Assumption 5.2. For a given compact set $\mathcal{Z} \subset \mathbb{R}^{n_z}$, the function $J(z)$ satisfy

- The derivative $\nabla_z J(z)$ is L_1 -Lipschitz, i.e., for any $z, z' \in \mathcal{Z}$, $\|\nabla_z J(z) - \nabla_z J(z')\| \leq L_1 \|z - z'\|$.
- The derivative $\nabla_{\theta} \nabla_u J(z)$ is L_2 -Lipschitz, i.e., for any $z, z' \in \mathcal{Z}$, $\|\nabla_{\theta} \nabla_u J(z) - \nabla_{\theta} \nabla_u J(z')\| \leq L_2 \|z - z'\|$.
- The derivative $\nabla_u^2 J(z)$ is L_3 -Lipschitz, i.e., for any $z, z' \in \mathcal{Z}$, $\|\nabla_u^2 J(z) - \nabla_u^2 J(z')\| \leq L_3 \|z - z'\|$.

Assumption 5.2 is widely adopted in optimization analysis (Ji et al., 2021; Ghadimi & Wang, 2018). Assumption 5.2 captures the Lipschitz properties of the unrolled cost function associated with the optimization-based policy. As our control policy is defined as an optimization, Assumptions 5.1 and 5.2 enable us to estimate the boundedness of $\nabla_{\theta} \log \pi_{\theta}(u_t | x_t)$. Next, as we propose to leverage policy gradients to optimize our policy parameters, we assume standard conditions within the policy optimization (Papini et al., 2018), regarding the initial state distribution and the trajectory cost.

Assumption 5.3. The initial state distribution \mathcal{D} is supported in a region with a finite radius D_0 . For any initial state $x_0 \sim \mathcal{D}$, the trajectory cost $L(\tau)$ is bounded, i.e., there exists a positive constant M such that $L(\tau) \leq M$.

We construct a compact set \mathcal{Z} in Assumption 5.2 as follows: (1) For any initial parameter $\theta^{(0)} \in \mathbb{R}^d$, we define a compact set $\mathcal{G}_{\theta} = \{\theta \mid \|\theta - \theta^{(0)}\|^2 \leq \Delta_0\}$ where $\Delta_0 > 0$. (2) Given the initial state distribution \mathcal{D} on a bounded domain, x_0 is bounded. For $\theta \in \mathcal{G}_{\theta}$, both the optimal actions u_t^{\star} from convex optimization and sampled actions u_t from truncated Gaussian are bounded. Therefore, by the boundedness of x_0 and u_t , all subsequent states x_t remain bounded. Let \mathcal{B}_x and \mathcal{B}_u be the compact sets containing all possible states and actions. We define $\mathcal{Z} = \mathcal{B}_x \times \mathcal{B}_u \times \mathcal{G}_{\theta}$, which is compact as it is the Cartesian product of compact sets. Now we can characterize the convergence of the proposed algorithm 1.

Theorem 5.4. Suppose Assumptions 5.1, 5.2 and 5.3 hold. For any $\epsilon > 0$, and $\nu \in (0, 1)$, define a smoothness constant

$$L_C = M \left(\frac{\sqrt{m}\beta T(L_2\mu^2 + L_1L_2\mu + L_1L_3\mu + L_1^2L_3)}{\mu^3} + \frac{L_1^2T}{\mu^2\sigma^2} + \frac{m\beta^2L_1^2T^2}{\mu^2} \right),$$

a stepsize $\eta = \frac{1}{4L_C}$, the number of policy iterations K , and the number of sampled trajectories for each policy gradient step $N = \frac{2m\beta^2M^2T^2L_1^2}{\epsilon^2\mu^2} \log \frac{2Kd}{\nu}$. Then, with probability at least $1 - \nu$, we have

$$\min_{k=0, \dots, K-1} \|\nabla_{\theta} C(\theta^{(k)})\|^2 \leq \frac{16L_C(C(\theta^{(0)}) - C(\bar{\theta}))}{K} + 3\epsilon. \quad (10)$$

where $\bar{\theta}$ is the global optimum of (3).

Proof. Proven in Appendix C. \square

Theorem 5.4 provides convergence guarantees for the proposed optimization-based control policy. In general, $C(\theta)$ is non-convex w.r.t. θ . In particular, even for linear system dynamics with quadratic cost, the function $C(\theta)$ can be non-convex w.r.t. the policy parameters θ (a specific example is given in Appendix C.1). Thus, the above convergence results in (10) ensure that the obtained policy is an δ -accurate stationary point for the objective function $C(\theta)$, where $\delta = \frac{16L_C(C(\theta^{(0)})-C(\bar{\theta}))}{K} + 3\epsilon$. To the best of our knowledge, this is the first non-asymptotic convergence result for optimization-based policy in policy gradient setting that provides the sample complexity guarantees.

Remark 1. Outline of Proof Idea. The detailed proof of Theorem 5.4 is provided in Appendix C.2. The main proof idea bridges the convergence of bilevel optimization and the policy gradient framework. We first leverage analysis in bilevel optimization (Ji et al., 2021; Kwon et al., 2023) to demonstrate the properties of the optimal action with respect to policy parameters when solving the optimization-based policy. This allows us to establish the boundedness of $\nabla_{\theta} \log \pi_{\theta}(u_t|x_t)$, which is crucial for ensuring the convergence of the policy gradient framework. Next, we utilize the convergence analysis from policy optimization (Papini et al., 2018; Yang et al., 2021) to demonstrate the smoothness of $C(\theta)$ and the convergence of the policy gradient algorithm. Our work contributes to this field by establishing a theoretical foundation for the convergence of the optimization-based policy and providing practical insights into how the two methods can be effectively combined. An interesting future direction includes exploring improved sample complexity for learning the optimization-based policy.

Remark 2. The strongly convexity assumption in Convergence Analysis. In the convergence analysis, we assume that the policy objective is strongly convex. For this property, a sufficient condition is that the cost function is strongly convex with respect to u and the dynamic function is convex and non-decreasing. We note that one can follow work (Chen et al., 2019b) to expand decision variable $\hat{u} = [u \ -u]$ to allow dynamic function to be convex without the non-decreasing requirement. Additionally, incorporating penalty terms, such as quadratic terms for state and action constraints, into the objective can further ensure strong convexity. This property frequently arises in applications like linear-quadratic regulators (LQR), portfolio optimization, and energy management systems. To the best of our knowledge, we are the first to provide a non-asymptotic convergence analysis for optimization policies. Extending the theoretical analysis to more general optimization-based policies is a promising direction for future work.

6. Experiments

We conclude with case studies demonstrating the effectiveness of DiffOP on both nonlinear dynamical systems (Cartpole, Robot arm, and Quadrotor) and a real-world building control problem. Detailed problem formulation, simulation setting, as well as implementation, are provided in Appendix D.

6.1. Nonlinear System Control

We compare our approach to the following approaches:

- Two optimization-based policies: (1) Pontryagin differentiable programming (PDP control) (Jin et al., 2020): while originally designed to learn from expert demonstrations, we extend it to learn from online interactions through trajectory loss minimization. (2) MPC-ICNN (Chen et al., 2019b): this approach uses input convex neural networks (ICNN) (Amos et al., 2017) to model system dynamics and implement a convex optimization policy. The model is trained *offline* to minimize prediction errors.
- Model-free reinforcement learning: PPO (Schulman et al., 2017), a widely-used RL algorithm that optimizes policies via proximal policy optimization.

For DiffOP, the dynamic model is characterized by an ICNN, and the control objective is modeled as a quadratic objective with unknown parameters Q, q, Q_H, q_H .

$$\begin{aligned} \min \quad & \sum_{i=0}^{H-1} \tau_i^T Q \tau_i + q^T \tau_i + x_H^T Q_H x_H + q_H^T x_H \\ \text{s.t.} \quad & x_{i+1} = x_i + \Delta t \cdot f_{\text{ICNN}}(x_i, u_i) \end{aligned} \quad (11)$$

with $\tau_i = [x_i \ u_i]$, and the discretization interval $\Delta t = 0.05s$ for cartpole and $\Delta t = 0.1s$ for robotarm and quadrotor. While both PDP control and MPC-ICNN use *true* cost functions, they learn dynamics from data. PDP control iteratively updates its dynamics model through environment interactions. We evaluate across five independent trials, each collecting batches of $N = 10$ trajectories.

Table 1 compares the final control costs achieved by each method across all tasks. DiffOP demonstrates strong performance across all nonlinear control tasks. In the cartpole system, it achieves comparable results to PDP. For Robotarm, DiffOP matches the optimal cost, outperforming all baselines. In the challenging Quadrotor task, DiffOP achieves 9% improvement over optimization policy baselines. Notably, DiffOP consistently shows smaller standard deviations, indicating more stable performance across all tasks. Figure 2 presents the control cost curves for all methods across three nonlinear control tasks. DiffOP combines

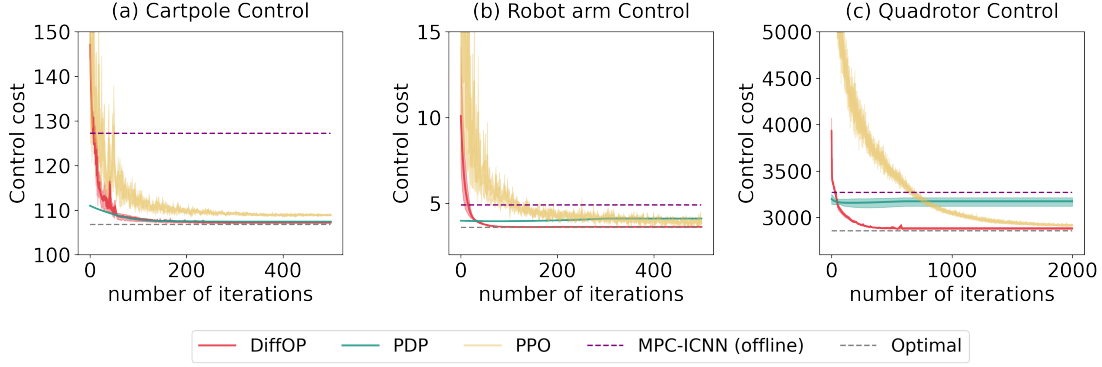


Figure 2. Control cost v.s. iteration for nonlinear system control. The solid line represents the mean cost of 5 experiments and shadow represents the 20/80 percentiles.

the strengths of both optimization-based and learning-based approaches. Optimization-based methods, such as PDP-control and MPC-ICNN, achieve low control costs in the early stages but are constrained by their indirect objectives of minimizing trajectory loss, limiting their final performance. On the other hand, model-free methods like PPO require longer training times and often converge to suboptimal solutions. By directly optimizing control cost while preserving sample efficiency, DiffOP bridges this gap, delivering superior final performance without compromising early-stage learning speed.

Table 1. Control cost on nonlinear control tasks.

Method	Control tasks		
	Cartpole	Robotarm	Quadrotor
PDP	107.4±0.0	4.1±0.03	3175.2 ±50.2
MPC-ICNN	127.2	4.9	3270.9
PPO	108.8±0.2	3.9±0.03	2920.2±14.8
DiffOP	107.3±0.2	3.6±0.02	2882.9±8.5
Optimal	106.8	3.6	2857.0

6.2. Building Control

We demonstrate DiffOP’s application to real-world building thermal control problem (Chen et al., 2019a) with a water-based radiant heating system. The system, modeled in EnergyPlus (Crawley et al., 2001) aims to optimize supply-water temperature for thermal comfort and energy efficiency of the building system. The challenge of building control lies in the fact that the relationship between the state/action and energy consumption is complex and difficult to model directly (Balaji et al., 2013), and the exact system dynamics are often unknown. Generally, researchers use the L1-norm of control actions as a proxy for energy consumption (Chen et al., 2019a;b). However, it may not accurately reflect the

actual energy consumption. In DiffOP, we use ICNN θ_{ICNN} to model the energy consumption cost function, and use a linear model θ_f to represent the dynamics. Our policy is defined as

$$\arg \min \sum_{i=0}^H (c(x_i, u_i; \theta_{\text{ICNN}}) + \alpha_{1,i}(x_i - x^*)^2),$$

$$\text{s.t. } x_{i+1} = \theta_f^T [x_i \ u_i \ d_i], \underline{u} \leq u_i \leq \bar{u},$$

where $x_i \in \mathbb{R}^1$ is zone temperature, $u_i \in \mathbb{R}^1$ is supply water temperature, $d_i \in \mathbb{R}^7$ represents the disturbance variables (e.g., outdoor temperature, outdoor air relative humidity, occupancy flag). $\alpha_{1,i} = \alpha$ when there is occupancy at the i -th step, where α is a learnable parameter, and $\alpha_{1,i} = 0$ when there is no occupancy. By incorporating $\alpha_{1,i}$, we dynamically adjust the objective function to consider occupant comfort only when relevant. The cost model parameters $\theta_c = (\theta_{\text{ICNN}}, \alpha_1)$ include the parameters of ICNN and weight coefficient α_1 , the dynamic model parameters are $\theta_f \in \mathbb{R}^{(n+m+p) \times n}$. Thermal comfort is measured by $(x_i - x^*)^2$ where x^* is the temperature setpoint and \underline{u}, \bar{u} denote the minimum and maximum supply water temperature.

We compare our approach against MPC-ICNN and PPO. Additionally, to address the limitations of PDP control in handling system disturbances, we introduce MPC-ICNN (traj), which adapts both cost and dynamic models by minimizing trajectory prediction errors.

First, we collect expert state-action demonstrations using the built-in controller under Typical Meteorological Year 3 (TMY3) weather sequence (Wilcox & Marion, 2008) from January 1st to March 31st, 2017. We initialize DiffOP and PPO using behavioral cloning on these demonstrations, while MPC-ICNN is initialized by minimizing dynamic model prediction loss. This initialization strategy allows all algorithms to leverage existing control knowledge effectively. We then deploy all the control methods on the simulation period spans from January 1st to March 31st,

2017, using the actual weather sequence. In the experiment, each natural day is considered as an episode, and we update the policy every single day. We provided the agent with ground truth information on future disturbances, i.e. weather and occupancy (Chen et al., 2019a).

Results are shown in Table 2, where predicted percent dissatisfied (PPD) and energy are calculated by Energy-Plus. PPD is a thermal comfort metric representing the percentage of dissatisfied occupants, by considering environmental and occupant parameters. Control cost is defined as $c(x_t, u_t) = \text{Energy demand(kW)}_t + \alpha_t \text{PPD}(\%)_t$, with $\alpha_t = 1$ during occupied periods and each control step is 15 minutes.

Table 2. Control performance on building control task.

Method	Mean PPD(%)	Total Energy(kWh)
MPC-ICNN	17.71	10673.3
MPC-ICNN(traj)	17.80	10624.1
PPO	18.76	12433.3
DiffOP	17.59	10575.8
Built in	17.78	11844.8

We observe that DiffOP outperformed all baseline methods by achieving the lowest PPD and lowest energy consumption. Specifically, the proposed DiffOP algorithm achieved 10.7% energy savings compared to the built-in controller while improving thermal comfort levels by reducing PPD.

Further, Figure 3 illustrates the control cost reduction achieved by DiffOP compared to DiffOP (offline trained). The results demonstrate the evolving performance of DiffOP through daily policy updates from January to March. The control cost reduction pattern shows a clear learning trend, with the magnitude of improvements generally increasing over time - from initial gains of 2-5 in terms of control cost in January to achieving peaks of over 20 by March.

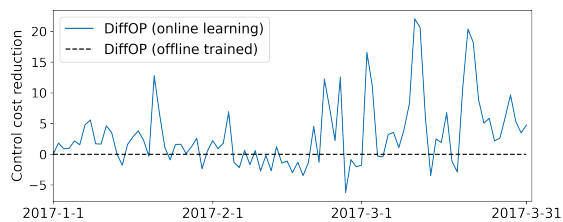


Figure 3. Control cost reduction achieved by DiffOP over time (higher values indicate better performance).

To illustrate the superior performance of DiffOP, Figure 4 compares control, indoor temperature and energy profiles. The pink-shaded area highlights nighttime control strategies: the built-in controller maintains unnecessary indoor temperature regulation during unoccupied hours, and PPO

exhibits oscillations in its control signals. Both patterns result in excessive energy consumption, as shown in the bottom figure (pink area). However, both optimization-based policies, DiffOP and MPC-ICNN, improve energy efficiency by reducing the supply air temperature through predictive planning. This forward-looking capacity also ensures effective morning temperature management, as shown in the green-shaded area, where DiffOP and MPC-ICNN preheat the room in anticipation of occupancy.

Compared to optimization policy, i.e., MPC-ICNN, DiffOP aligns with the built-in controller’s efficiency in estimating preheating requirements, leading to reduced energy consumption. In contrast, MPC-ICNN exhibits less smooth control actions during daytime operation, leading to inefficient energy consumption.

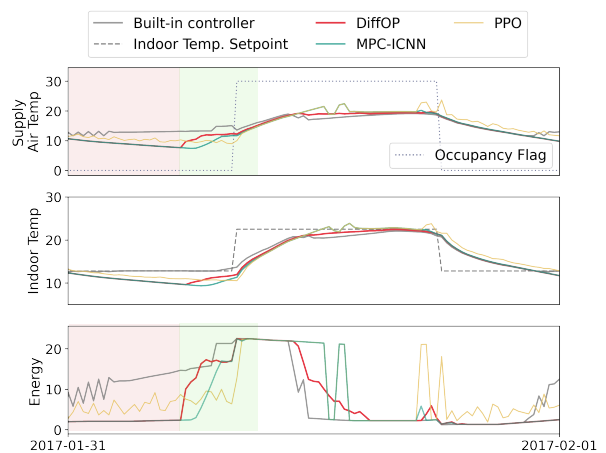


Figure 4. Control action, indoor temperature and energy profiles for building control task.

7. Conclusion

This paper proposes DiffOP, a differentiable optimization-based control policy that learns both the cost model and dynamic model using policy gradients through direct interaction with the environment. This work first presents the non-asymptotic convergence results for learning an optimization-based policy with a policy gradient algorithm. Furthermore, the numerical results demonstrate that our approach can reduce the actual control costs, achieving lower costs compared to both model-based and model-free control policies.

This work opens the door to several interesting directions for future research. First, we aim to explore improved sample complexity for learning the optimization-based policy. Secondly, it would be of significant interest to further investigate the interpretability and robustness of our approach in comparison to traditional control policies. Finally, we envision extending the experimental results of DiffOP to a wide range of real-world deployments.

Impact Statement

This work advances policy optimization for real-world control applications by developing a theoretically-grounded framework for optimization-based policies. Our approach enables reliable and efficient policy learning, validated through both numerical simulations and building control experiment without requiring prior system knowledge. We envision our framework will improve the performance of robotic systems, industrial automation, and other practical optimization applications.

References

- Agarwal, A., Kakade, S. M., Lee, J. D., and Mahajan, G. Optimality and approximation with policy gradient methods in markov decision processes. In *Conference on Learning Theory*, pp. 64–66. PMLR, 2020.
- Agrawal, A., Amos, B., Barratt, S., Boyd, S., Diamond, S., and Kolter, J. Z. Differentiable convex optimization layers. *Advances in neural information processing systems*, 32, 2019.
- Amos, B. and Kolter, J. Z. Optnet: Differentiable optimization as a layer in neural networks. In *International conference on machine learning*, pp. 136–145. PMLR, 2017.
- Amos, B., Xu, L., and Kolter, J. Z. Input convex neural networks. In *International Conference on Machine Learning*, pp. 146–155. PMLR, 2017.
- Amos, B., Jimenez, I., Sacks, J., Boots, B., and Kolter, J. Z. Differentiable mpc for end-to-end planning and control. *Advances in neural information processing systems*, 31, 2018.
- Andersson, J. A. E., Gillis, J., Horn, G., Rawlings, J. B., and Diehl, M. CasADi – A software framework for nonlinear optimization and optimal control. *Mathematical Programming Computation*, 11(1):1–36, 2019. doi: 10.1007/s12532-018-0139-4.
- Balaji, B., Teraoka, H., Gupta, R., and Agarwal, Y. Zonepac: Zonal power estimation and control via hvac metering and occupant feedback. In *Proceedings of the 5th ACM Workshop on Embedded Systems For Energy-Efficient Buildings*, pp. 1–8, 2013.
- Bertsekas, D. P. *Constrained optimization and Lagrange multiplier methods*. Academic press, 2014.
- Chen, B., Cai, Z., and Bergés, M. Gnu-rl: A precocial reinforcement learning solution for building hvac control using a differentiable mpc policy. In *Proceedings of the 6th ACM international conference on systems for energy-efficient buildings, cities, and transportation*, pp. 316–325, 2019a.
- Chen, Y., Shi, Y., and Zhang, B. Optimal control via neural networks: A convex approach. In *International Conference on Learning Representations*, 2019b.
- Crawley, D. B., Lawrie, L. K., Winkelmann, F. C., Buhl, W. F., Huang, Y. J., Pedersen, C. O., Strand, R. K., Liesen, R. J., Fisher, D. E., Witte, M. J., et al. Energyplus: creating a new-generation building energy simulation program. *Energy and buildings*, 33(4):319–331, 2001.
- Diamond, S. and Boyd, S. Cvxpy: A python-embedded modeling language for convex optimization. *Journal of Machine Learning Research*, 17(83):1–5, 2016.
- Donti, P., Amos, B., and Kolter, J. Z. Task-based end-to-end model learning in stochastic optimization. *Advances in neural information processing systems*, 30, 2017.
- Drgoña, J., Tuor, A., and Vrabie, D. Learning constrained parametric differentiable predictive control policies with guarantees. *IEEE Transactions on Systems, Man, and Cybernetics: Systems*, 2024.
- Elmachtoub, A. N. and Grigas, P. Smart “predict, then optimize”. *Management Science*, 68(1):9–26, 2022.
- Eysenbach, B., Khazatsky, A., Levine, S., and Salakhutdinov, R. R. Mismatched no more: Joint model-policy optimization for model-based rl. *Advances in Neural Information Processing Systems*, 35:23230–23243, 2022.
- Fazel, M., Ge, R., Kakade, S., and Mesbahi, M. Global convergence of policy gradient methods for the linear quadratic regulator. In *International conference on machine learning*, pp. 1467–1476. PMLR, 2018.
- Ghadimi, S. and Wang, M. Approximation methods for bilevel programming. *arXiv preprint arXiv:1802.02246*, 2018.
- Giegrich, M., Reisinger, C., and Zhang, Y. Convergence of policy gradient methods for finite-horizon exploratory linear-quadratic control problems. *SIAM Journal on Control and Optimization*, 62(2):1060–1092, 2024.
- Gill, P. E., Murray, W., and Saunders, M. A. Snpot: An sqp algorithm for large-scale constrained optimization. *SIAM review*, 47(1):99–131, 2005.
- Gould, S., Hartley, R., and Campbell, D. Deep declarative networks. *IEEE Transactions on Pattern Analysis and Machine Intelligence*, 44(8):3988–4004, 2021.
- Grathwohl, W., Choi, D., Wu, Y., Roeder, G., and Duvenaud, D. Backpropagation through the void: Optimizing control variates for black-box gradient estimation. *arXiv preprint arXiv:1711.00123*, 2017.

- Gros, S. and Zanon, M. Data-driven economic nmPC using reinforcement learning. *IEEE Transactions on Automatic Control*, 65(2):636–648, 2019.
- Gros, S. and Zanon, M. Reinforcement learning based on MPC and the stochastic policy gradient method. In *2021 American Control Conference (ACC)*, pp. 1947–1952. IEEE, 2021.
- Grüne, L., Pannek, J., Grüne, L., and Pannek, J. *Nonlinear model predictive control*. Springer, 2017.
- Hao, W., Heredia, P. C., Huang, B., Lu, Z., Liang, Z., and Mou, S. Policy learning based on deep koopman representation. *arXiv preprint arXiv:2305.15188*, 2023.
- Jain, A., Chan, L., Brown, D. S., and Dragan, A. D. Optimal cost design for model predictive control. In *Learning for Dynamics and Control*, pp. 1205–1217. PMLR, 2021.
- Ji, K., Yang, J., and Liang, Y. Bilevel optimization: Convergence analysis and enhanced design. In *International conference on machine learning*, pp. 4882–4892. PMLR, 2021.
- Jin, W., Wang, Z., Yang, Z., and Mou, S. Pontryagin differentiable programming: An end-to-end learning and control framework. *Advances in Neural Information Processing Systems*, 33:7979–7992, 2020.
- Killian, M. and Kozek, M. Ten questions concerning model predictive control for energy efficient buildings. *Building and Environment*, 105:403–412, 2016.
- Kwon, J., Kwon, D., Wright, S., and Nowak, R. D. A fully first-order method for stochastic bilevel optimization. In *International Conference on Machine Learning*, pp. 18083–18113. PMLR, 2023.
- Lambert, N., Amos, B., Yadan, O., and Calandra, R. Objective mismatch in model-based reinforcement learning. *arXiv preprint arXiv:2002.04523*, 2020.
- Machowski, J., Lubosny, Z., Bialek, J. W., and Bumby, J. R. *Power system dynamics: stability and control*. John Wiley & Sons, 2020.
- Mandi, J., Kotary, J., Berden, S., Mulamba, M., Bucarey, V., Guns, T., and Fioretto, F. Decision-focused learning: Foundations, state of the art, benchmark and future opportunities. *Journal of Artificial Intelligence Research*, 80:1623–1701, 2024.
- Morari, M. and Lee, J. H. Model predictive control: past, present and future. *Computers & chemical engineering*, 23(4-5):667–682, 1999.
- Negenborn, R. R., De Schutter, B., and Hellendoorn, J. Multi-agent model predictive control for transportation networks: Serial versus parallel schemes. *Engineering Applications of Artificial Intelligence*, 21(3):353–366, 2008.
- Okada, M., Rigazio, L., and Aoshima, T. Path integral networks: End-to-end differentiable optimal control. *arXiv preprint arXiv:1706.09597*, 2017.
- Papini, M., Binaghi, D., Canonaco, G., Pirota, M., and Restelli, M. Stochastic variance-reduced policy gradient. In *International conference on machine learning*, pp. 4026–4035. PMLR, 2018.
- Pineda, L., Fan, T., Monge, M., Venkataraman, S., Sodhi, P., Chen, R. T., Ortiz, J., DeTone, D., Wang, A., Anderson, S., et al. Theseus: A library for differentiable nonlinear optimization. *Advances in Neural Information Processing Systems*, 35:3801–3818, 2022.
- Raffin, A., Hill, A., Gleave, A., Kanervisto, A., Ernestus, M., and Dormann, N. Stable-baselines3: Reliable reinforcement learning implementations. *Journal of Machine Learning Research*, 22(268):1–8, 2021. URL <http://jmlr.org/papers/v22/20-1364.html>.
- Rudin, W. et al. *Principles of mathematical analysis*, volume 3. McGraw-hill New York, 1964.
- Scherrer, B. Approximate policy iteration schemes: A comparison. In *International Conference on Machine Learning*, pp. 1314–1322. PMLR, 2014.
- Schulman, J., Wolski, F., Dhariwal, P., Radford, A., and Klimov, O. Proximal policy optimization algorithms. *arXiv preprint arXiv:1707.06347*, 2017.
- Spong, M. W. and Vidyasagar, M. *Robot dynamics and control*. John Wiley & Sons, 2008.
- Spong, M. W., Hutchinson, S., and Vidyasagar, M. *Robot modeling and control*. John Wiley & Sons, 2020.
- Sutton, R. S. and Barto, A. G. *Reinforcement learning: An introduction*. MIT press, 2018.
- Sutton, R. S., McAllester, D., Singh, S., and Mansour, Y. Policy gradient methods for reinforcement learning with function approximation. *Advances in neural information processing systems*, 12, 1999.
- Vemula, A., Song, Y., Singh, A., Bagnell, D., and Choudhury, S. The virtues of laziness in model-based RL: A unified objective and algorithms. In *International Conference on Machine Learning*, pp. 34978–35005. PMLR, 2023.

- Wan, W., Wang, Y., Erickson, Z., and Held, D. Difftop: Differentiable trajectory optimization for deep reinforcement and imitation learning. *arXiv preprint arXiv:2402.05421*, 2024.
- Wilcox, S. and Marion, W. Users manual for tmy3 data sets. 2008.
- Xu, M., Molloy, T. L., and Gould, S. Revisiting implicit differentiation for learning problems in optimal control. *Advances in Neural Information Processing Systems*, 36, 2024.
- Xu, T., Liang, Y., and Lan, G. Crpo: A new approach for safe reinforcement learning with convergence guarantee. In *International Conference on Machine Learning*, pp. 11480–11491. PMLR, 2021.
- Yang, L., Zheng, Q., and Pan, G. Sample complexity of policy gradient finding second-order stationary points. In *Proceedings of the AAAI Conference on Artificial Intelligence*, volume 35, pp. 10630–10638, 2021.
- Zhang, Z. and Lam, K. P. Practical implementation and evaluation of deep reinforcement learning control for a radiant heating system. In *Proceedings of the 5th Conference on Systems for Built Environments*, pp. 148–157, 2018.
- Zhao, T., Hachiya, H., Niu, G., and Sugiyama, M. Analysis and improvement of policy gradient estimation. *Advances in Neural Information Processing Systems*, 24, 2011.

Appendix

A. Analytical form of policy gradients

Here we proof for proposition 4.1.

Proof. With (4):

$$u_t \sim \pi_\theta(u|x_t) = \frac{\phi(u|u_t^*, \sigma^2 I)}{\int_{u_t^* - \beta\sigma^2 I}^{u_t^* + \beta\sigma^2 I} \phi(u|u_t^*, \sigma^2 I) du},$$

we have

$$\pi_\theta(u|x_t) = \frac{1}{Z(2\pi)^{\frac{m}{2}} |\sigma^2 I|^{\frac{1}{2}}} \exp\left(-\frac{1}{2\sigma^2} (u_t - u_t^*)^\top (u_t - u_t^*)\right),$$

where Z is a normalization constant, i.e., the integral of the multivariate Gaussian PDF over the truncated range

$$Z = \int_{u_t^* - \beta\sigma^2 I}^{u_t^* + \beta\sigma^2 I} \phi(u|u_t^*, \sigma^2 I) du.$$

The derivative of the log probability is

$$\nabla_\theta \log \pi_\theta(u|x_t) = \frac{1}{\sigma^2} [\nabla_\theta u_t^*]^\top (u_t - u_t^*),$$

where u_t is the action applied to the system at time t , u_t^* is the corresponding optimal solution. In conjunction with $\nabla_\theta C(\theta) = \mathbb{E}[L(\tau) \nabla_\theta \log \pi_\theta(\tau)]$, we obtain

$$\nabla_\theta C(\theta) = \mathbb{E} \left[L(\tau) \left(\sum_{t=0}^T \frac{1}{\sigma^2} \nabla_\theta u_t^*{}^\top (u_t - u_t^*) \right) \right].$$

□

B. Proof for Gradient of the optimization-based policy

Proof. Let $\lambda \in \mathbb{R}^{n_\kappa}$ and denote $\lambda_{i,j}$ as the dual variable corresponding to the j -th element of κ_i . By the method of Lagrange multipliers (Bertsekas, 2014), we form the Lagrangian:

$$L(\theta, \zeta, \lambda) = J(\zeta; \theta) - \sum_{i=-1}^H \sum_{j=1}^{|\kappa_i|} \lambda_{i,j} [\kappa_i(\zeta; \theta)]_j.$$

Since the ζ^* is the optimal solution, we have

$$\left[\nabla_\zeta J(\zeta^*; \theta) - \sum_{i=-1}^H \sum_{j=1}^{|\kappa_i|} \lambda_{i,j} \nabla_\zeta [\kappa_i(\zeta^*; \theta)]_j \right] = 0. \quad (12)$$

For the first row in equation (12), we have

$$\nabla_\zeta J(\zeta^*; \theta) = \sum_{i=-1}^H \sum_{j=1}^{|\kappa_i|} \lambda_{i,j} \nabla_\zeta [\kappa_i(\zeta^*; \theta)]_j = \lambda^\top A, \quad (13)$$

for A defined as $A = \nabla_\zeta \kappa(\zeta^*; \theta)$. In the following statement, we simplify $[\kappa_i(\zeta^*; \theta)]_j$ as $[\kappa_i]_j$ and $J(\zeta^*; \theta)$ as J . Then, differentiating the gradient of the Lagrangian with respect to θ we have

$$\left[\begin{array}{c} \nabla_{\theta\zeta}^2 J + \nabla_\zeta^2 J \nabla_\theta \zeta^* - \nabla_\zeta \kappa^\top \nabla_\theta \lambda - \sum_{i=-1}^H \sum_{j=1}^{|\kappa_i|} \lambda_{i,j} \left(\nabla_{\theta\zeta}^2 [\kappa_i]_j + \nabla_\zeta^2 [\kappa_i]_j \nabla_\theta \zeta^* \right) \\ \nabla_\theta \kappa + \nabla_\zeta \kappa \nabla_\theta \zeta^* \end{array} \right] = 0. \quad (14)$$

Therefore, we have

$$\begin{bmatrix} \nabla_{\zeta}^2 J - \sum_{i=-1}^H \sum_{j=1}^{|\kappa_i|} \lambda_{ij} \nabla_{\zeta}^2 [\kappa_i]_j & -\nabla_{\zeta} \kappa^{\top} \\ \nabla_{\zeta} \kappa & 0 \end{bmatrix} \begin{bmatrix} \nabla_{\theta} \zeta^* \\ \nabla_{\theta} \lambda \end{bmatrix} = - \begin{bmatrix} \nabla_{\theta \zeta}^2 J - \sum_{i=-1}^H \sum_{j=1}^{|\kappa_i|} \lambda_{i,j} \nabla_{\theta \zeta}^2 [\kappa_i]_j \\ \nabla_{\theta} \kappa \end{bmatrix} \quad (15)$$

where all functions are evaluated at (ζ^*, θ) . Then we can solve $\nabla_{\theta} \zeta^*$ with

$$\nabla_{\theta} \zeta^* = D^{-1} A^{\top} (AD^{-1} A^{\top})^{-1} (AD^{-1} B - C) - D^{-1} B.$$

Since $\nabla_{\theta} \zeta^* = [\nabla_{\theta} x_0^*, \nabla_{\theta} u_0^*, \dots, \nabla_{\theta} x_{H-1}^*, \nabla_{\theta} u_{H-1}^*, \nabla_{\theta} X_H^*]$. After evaluating $\nabla_{\theta} \zeta^*$, we have

$$\nabla_{\theta} u_0^* = [\nabla_{\theta} \zeta^*]_{n:n+m}.$$

□

C. Convergence results of the Proposed Framework

C.1. Non-convexity of $C(\theta)$

In this subsection, we provide an example demonstrating that $C(\theta)$ is non-convex even for simple LQR problems. We consider both the state and action as scalars, with $x \in \mathbb{R}$ and $u \in \mathbb{R}$. The problem is formulated as

$$C(\theta) = \sum_{t=1}^T x_t^2 + u_t^2, \text{ s.t. } x_1 = 5, x_{t+1} = x_t - 0.5u_t, u_{1:T} = \pi(u; \theta), \quad (16)$$

where $T = 6$, and the policy is formulated as

$$\pi(u; \theta) := \min_u \sum_{i=1}^T \theta_1 x_i^2 + \theta_2 u_i^2, \text{ s.t. } x_1 = 5, x_{i+1} = \theta_3 x_i + \theta_4 u_i. \quad (17)$$

Let $\theta^{(1)} = [1, 1, 2, -0.5]$, $\theta^{(2)} = [2, 1, 2, -0.5]$, there exists $\alpha \in (0, 1)$ (for instance $\alpha = 0.5$), such that $C(\alpha\theta^{(1)} + (1 - \alpha)\theta^{(2)}) > \alpha C(\theta^{(1)}) + (1 - \alpha)C(\theta^{(2)})$.

C.2. Proof of Theorem 5.4

In what follows, we make the parameter dependency explicit by writing $u^*(\theta)$ (instead of u^*) to facilitate the gradient analysis. To prove Theorem 5.4, we first characterize the Lipschitz properties of $u^*(\theta)$ and $\nabla_{\theta} u^*(\theta)$ in Lemma C.1. Then we can bound the policy derivatives which is sufficient for the L-smoothness of the objective $C(\theta)$. Finally, we prove the convergence of our policy gradient algorithm.

Here, we characterize the Lipschitz properties of $u^*(\theta)$ and $\nabla_{\theta} u^*(\theta)$.

Lemma C.1. *Suppose Assumptions 5.1 and 5.2 hold and define the implicit function $u^* : \theta \rightarrow u^*(\theta), \forall \theta \in \mathcal{G}_{\theta}$. We have*

- $\|\nabla_{\theta} u^*(\theta)\| \leq \frac{L_1}{\mu}$.
- $\|\nabla_{\theta}^2 u^*(\theta)\| \leq \frac{L_2}{\mu} + \frac{L_1 L_2 + L_1 L_3}{\mu^2} + \frac{L_1^2 L_3}{\mu^3}$.

Proof. The implicit function is defined as

$$u^*(\theta) = \min_u J(x_{\text{init}}, u, \theta).$$

Due to the optimality condition, we have $\nabla_u J(x_{\text{init}}, u^*(\theta), \theta) = 0$. By taking derivative on both sides, using the chain rule and the implicit function theorem (Rudin et al., 1964), we obtain

$$\nabla_{\theta} \nabla_u J(x_{\text{init}}, u^*(\theta), \theta) + \nabla_u^2 J(x_{\text{init}}, u^*(\theta), \theta) \nabla_{\theta} u^*(\theta) = 0.$$

Let $z^* = (x_{\text{init}}, u^*(\theta), \theta)$, we have

$$\nabla_{\theta} u^*(\theta) = -[\nabla_u^2 J(z^*)]^{-1} [\nabla_{\theta} \nabla_u J(z^*)]. \quad (18)$$

As $J(x_{\text{init}}, u, \theta)$ is μ -strongly convex w.r.t. u , we have

$$\|\nabla_u^2 J(z^*)\|^{-1} \leq 1/\mu.$$

Additionally, as $\nabla_z J(z^*)$ is L_1 -Lipschitz, we have

$$\|\nabla_u J(z^*) - \nabla_u J(z^{*'})\| \leq \|\nabla_z J(z^*) - \nabla_z J(z^{*'})\| \leq L_1 \|z^* - z^{*'}\|.$$

Then $\nabla_u J(z^*)$ is L_1 -Lipschitz, its partial derivative is bounded by L_1 :

$$\|\nabla_{\theta} \nabla_u J(z^*)\| \leq L_1.$$

We obtain

$$\|\nabla_{\theta} u^*(\theta)\| \leq \|\nabla_u^2 J(z^*)\|^{-1} \|\nabla_{\theta} \nabla_u J(z^*)\| \leq \frac{L_1}{\mu}, \quad \|u^*(\theta) - u^*(\theta')\| \leq \frac{L_1}{\mu} \|\theta - \theta'\|.$$

For any $\theta, \theta' \in \mathbb{R}^d$, let $z^{*'} = (x_{\text{init}}, u^*(\theta'), \theta')$, we have

$$\begin{aligned} \|\nabla_{\theta} u^*(\theta) - \nabla_{\theta} u^*(\theta')\| &= \left\| -[\nabla_u^2 J(z^*)]^{-1} [\nabla_{\theta} \nabla_u J(z^*)] + [\nabla_u^2 J(z^*)]^{-1} [\nabla_{\theta} \nabla_u J(z^{*'})] \right. \\ &\quad \left. - [\nabla_u^2 J(z^*)]^{-1} [\nabla_{\theta} \nabla_u J(z^{*'})] + [\nabla_u^2 J(z^{*'})]^{-1} [\nabla_{\theta} \nabla_u J(z^{*'})] \right\| \\ &\leq \left\| -[\nabla_u^2 J(z^*)]^{-1} [\nabla_{\theta} \nabla_u J(z^*)] + [\nabla_u^2 J(z^*)]^{-1} [\nabla_{\theta} \nabla_u J(z^{*'})] \right\| \\ &\quad + \left\| -[\nabla_u^2 J(z^*)]^{-1} [\nabla_{\theta} \nabla_u J(z^{*'})] + [\nabla_u^2 J(z^{*'})]^{-1} [\nabla_{\theta} \nabla_u J(z^{*'})] \right\| \\ &\leq \left\| [\nabla_u^2 J(z^*)]^{-1} \right\| \|\nabla_{\theta} \nabla_u J(z^*) - \nabla_{\theta} \nabla_u J(z^{*'})\| \\ &\quad + \|\nabla_{\theta} \nabla_u J(z^{*'})\| \left\| [\nabla_u^2 J(z^*)]^{-1} - [\nabla_u^2 J(z^{*'})]^{-1} \right\| \\ &\leq \frac{1}{\mu} L_2 \|z^* - z^{*'}\| + L_1 \left\| [\nabla_u^2 J(z^*)]^{-1} - [\nabla_u^2 J(z^{*'})]^{-1} \right\|. \end{aligned} \quad (19)$$

Further, using the Lipschitz property of $\nabla_u^2 J(z^*)$ and boundness of $\|\nabla_u^2 J(z^*)\|$, we have

$$\begin{aligned} \left\| [\nabla_u^2 J(z^*)]^{-1} - [\nabla_u^2 J(z^{*'})]^{-1} \right\| &\leq \left\| [\nabla_u^2 J(z^*)]^{-1} \right\| \|\nabla_u^2 J(z^*) - \nabla_u^2 J(z^{*'})\| \left\| [\nabla_u^2 J(z^{*'})]^{-1} \right\| \\ &\leq \frac{L_3}{\mu^2} \|z^* - z^{*'}\|. \end{aligned} \quad (20)$$

We note

$$\|z^* - z^{*'}\| \leq \|\theta - \theta'\| + \|u^*(\theta) - u^*(\theta')\| \leq \frac{\mu + L_1}{\mu} \|\theta - \theta'\| \quad (21)$$

Combining equation (19),(20) and (21) yields

$$\|\nabla_{\theta} u^*(\theta) - \nabla_{\theta} u^*(\theta')\| \leq \left(\frac{L_2}{\mu} + \frac{L_1 L_2 + L_1 L_3}{\mu^2} + \frac{L_1^2 L_3}{\mu^3} \right) \|\theta - \theta'\|. \quad (22)$$

Following (22), we have

$$\|\nabla_{\theta}^2 u^*(\theta)\| \leq \frac{L_2}{\mu} + \frac{L_1 L_2 + L_1 L_3}{\mu^2} + \frac{L_1^2 L_3}{\mu^3}.$$

□

Lemma C.2 (Smoothness of $C(\theta)$). *Suppose Assumptions 5.1 and 5.2 hold. Then, we have, for any $\theta, \theta' \in \mathcal{G}_{\theta}$,*

$$\|\nabla_{\theta} C(\theta) - \nabla_{\theta} C(\theta')\| \leq L_C \|\theta - \theta'\|,$$

where the constant L_C is given by

$$L_C = M \left(\frac{\sqrt{m} \beta T (L_2 \mu^2 + L_1 L_2 \mu + L_1 L_3 \mu + L_1^2 L_3)}{\mu^3} + \frac{L_1^2 T}{\mu^2 \sigma^2} + \frac{m \beta^2 L_1^2 T^2}{\mu^2} \right).$$

Proof. We begin by establishing the boundedness of the gradient $\|\nabla_{\theta} \log \pi_{\theta}(u_t|x_t)\|$ and the Hessian $\|\nabla_{\theta}^2 \log \pi_{\theta}(u_t|x_t)\|$ w.r.t. θ .

Recall that

$$\pi_{\theta}(u_t|x_t) = \frac{1}{Z(2\pi)^{\frac{m}{2}}|\sigma^2 I|^{\frac{1}{2}}} \exp\left(-\frac{1}{2\sigma^2}(u_t - u_t^*(\theta))^{\top}(u_t - u_t^*(\theta))\right),$$

the gradient and the hessian are

$$\begin{aligned} \nabla_{\theta} \log \pi_{\theta}(u_t|x_t) &= \frac{1}{\sigma^2} \nabla_{\theta} u_t^*(\theta)^{\top} (u_t - u_t^*(\theta)), \\ \nabla_{\theta}^2 \log \pi_{\theta}(u_t|x_t) &= \frac{1}{\sigma^2} (\nabla_{\theta}^2 u_t^*(\theta)^{\top} (u_t - u_t^*(\theta)) - \nabla_{\theta} u_t^*(\theta)^{\top} \nabla_{\theta} u_t^*(\theta)). \end{aligned} \quad (23)$$

Recall that as we use the truncated Gaussian policy, we have

$$\begin{aligned} -\beta\sigma^2 &\leq [u_t^*]_i - [u_t]_i \leq \beta\sigma^2, i = 1, \dots, m \\ \Leftrightarrow \|u_t - u_t^*(\theta)\| &\leq \sqrt{m}\beta\sigma^2. \end{aligned} \quad (24)$$

In conjunction with lemma C.1, we obtain

$$\|\nabla_{\theta} \log \pi_{\theta}(u_t|x_t)\| \leq \frac{\sqrt{m}\beta\sigma^2}{\sigma^2} \|\nabla_{\theta} u_t^*(\theta)\| \leq \frac{\sqrt{m}\beta\sigma^2}{\sigma^2} \|\nabla_{\theta} u^*(\theta)\| \leq \frac{\sqrt{m}\beta L_1}{\mu} \quad (25)$$

and

$$\begin{aligned} \|\nabla_{\theta}^2 \log \pi_{\theta}(u_t|x_t)\| &\leq \frac{1}{\sigma^2} (\sqrt{m}\beta\sigma^2 \|\nabla_{\theta}^2 u_t^*(\theta)\| + \|\nabla_{\theta} u_t^*(\theta)\|^2) \\ &\leq \frac{1}{\sigma^2} (\sqrt{m}\beta\sigma^2 \|\nabla_{\theta}^2 u^*(\theta)\| + \|\nabla_{\theta} u^*(\theta)\|^2) \\ &\leq \sqrt{m}\beta \left(\frac{L_2}{\mu} + \frac{L_1 L_2 + L_1 L_3}{\mu^2} + \frac{L_1^2 L_3}{\mu^3} \right) + \frac{L_1^2}{\mu^2 \sigma^2}. \end{aligned} \quad (26)$$

Recall that $C(\theta) = \mathbb{E}_{\tau}[L(\tau)]$, we have

$$\nabla_{\theta} C(\theta) = \int_{\tau} L(\tau) \pi_{\theta}(\tau) \nabla_{\theta} \log \pi_{\theta}(\tau) d\tau. \quad (27)$$

By taking the derivative of (27), we obtain

$$\nabla_{\theta}^2 C(\theta) = \int_{\tau} (L(\tau) \pi_{\theta}(\tau) \nabla_{\theta}^2 \log \pi_{\theta}(\tau) + L(\tau) \pi_{\theta}(\tau) \nabla_{\theta} \log \pi_{\theta}(\tau) \nabla_{\theta} \log \pi_{\theta}(\tau)^{\top}) d\tau \quad (28)$$

In this case,

$$\nabla_{\theta} \log \pi_{\theta}(\tau) = \sum_{t=1}^T \nabla_{\theta} \log \pi_{\theta}(u_t|x_t), \quad \nabla_{\theta}^2 \log \pi_{\theta}(\tau) = \sum_{t=1}^T \nabla_{\theta}^2 \log \pi_{\theta}(u_t|x_t).$$

With equation (28) and Assumption 5.3, we have

$$\begin{aligned} \|\nabla_{\theta}^2 C(\theta)\| &\leq M \max(\|\nabla_{\theta}^2 \log \pi_{\theta}(\tau)\| + \|\nabla_{\theta} \log \pi_{\theta}(\tau)\|^2) \underbrace{\int_{\tau} \pi_{\theta}(\tau) d\tau}_{=1} \\ &\leq M \left(\frac{\sqrt{m}\beta T (L_2 \mu^2 + L_1 L_2 \mu + L_1 L_3 \mu + L_1^2 L_3)}{\mu^3} + \frac{L_1^2 T}{\mu^2 \sigma^2} + \frac{m\beta^2 L_1^2 T^2}{\mu^2} \right). \end{aligned} \quad (29)$$

Since the Hessian is bounded, for any $\theta, \theta' \in \mathcal{G}_{\theta}$, $C(\theta)$ satisfy

$$\|\nabla_{\theta} C(\theta) - \nabla_{\theta} C(\theta')\| \leq L_C \|\theta - \theta'\|, \quad (30)$$

where

$$L_C = M \left(\frac{\sqrt{m}\beta T(L_2\mu^2 + L_1L_2\mu + L_1L_3\mu + L_1^2L_3)}{\mu^3} + \frac{L_1^2T}{\mu^2\sigma^2} + \frac{m\beta^2L_1^2T^2}{\mu^2} \right).$$

□

We then characterize the gradient estimation error $\|\widehat{\nabla}_\theta C(\theta^{(k)}) - \nabla_\theta C(\theta^{(k)})\|$, where $\theta^{(k)}$ is the policy parameter at k -th iteration and $\widehat{\nabla}_\theta C$ is estimated by the REINFORCE estimator (score function gradient estimator).

Lemma C.3. *Suppose Assumptions 5.1, 5.2 and 5.3 hold. Then given e_{grad} , for any $\nu \in (0, 1)$, when $N \geq \frac{2m\beta^2M^2T^2L_1^2}{e_{grad}^2\mu^2} \log \frac{2d}{\nu}$, then with probability at least $1 - \nu$,*

$$\|\widehat{\nabla}_\theta C(\theta^{(k)}) - \nabla_\theta C(\theta^{(k)})\|^2 \leq e_{grad}. \quad (31)$$

Proof. Recall that

$$\nabla_\theta C(\theta) = \mathbb{E}[L(\tau)\nabla_\theta \log \pi_\theta(\tau)], \quad \widehat{\nabla}_\theta C(\theta) = \frac{1}{N} \sum_{i=1}^N L(\tau^{(i)})\nabla_\theta \log \pi_\theta(\tau^{(i)}).$$

Let $X_i = L(\tau^{(i)})\nabla_\theta \log \pi_\theta(\tau^{(i)})$. We have

$$\|X_i\| \leq \|L(\tau^{(i)})\nabla_\theta \log \pi_\theta(\tau^{(i)})\| \leq \|L(\tau^{(i)})\| \|\nabla_\theta \log \pi_\theta(\tau^{(i)})\| \leq \frac{\sqrt{m}\beta M T L_1}{\mu}, \quad (32)$$

where the third inequality we used equation (25).

Choose $N \geq \frac{2m\beta^2M^2T^2L_1^2}{e_{grad}^2\mu^2} \log \frac{2d}{\nu}$, and by Hoeffding's bound, with probability at least $1 - \nu$,

$$\|\widehat{\nabla}_\theta C(\theta^{(k)}) - \nabla_\theta C(\theta^{(k)})\|^2 \leq e_{grad}. \quad (33)$$

□

We now can provide proof for Theorem 5.4.

Proof for Theorem 5.4. Let \mathcal{F}_k be the filtration generated by $\{\widehat{\nabla}_\theta C(\theta^{(k')})\}_{k'=0}^{k-1}$. Then we have $\theta^{(k)}$ is \mathcal{F}_k measurable. We define the following event,

$$\mathcal{E}_k = \{\|\widehat{\nabla}_\theta C(\theta^{(k')}) - \nabla_\theta C(\theta^{(k')})\|^2 \leq e_{grad}, \forall k' = 0, 1, \dots, k-1\}, \quad (34)$$

and \mathcal{E}_k is also \mathcal{F}_k -measurable. By lemma C.3 and selection of $N \geq \frac{2m\beta^2M^2T^2L_1^2}{e_{grad}^2\mu^2} \log \frac{2Kd}{\nu}$, we have $\|\widehat{\nabla}_\theta C(\theta^{(k)}) - \nabla_\theta C(\theta^{(k)})\|^2 \leq e_{grad}$ with probability at least $1 - \frac{\nu}{K}$. Then we have

$$\mathbb{E}[\mathbf{1}(\mathcal{E}_{k+1})|\mathcal{F}_k]\mathbf{1}(\mathcal{E}_k) \geq (1 - \frac{\nu}{K})\mathbf{1}(\mathcal{E}_k). \quad (35)$$

Take expectation on both side, we obtain

$$\mathbb{P}(\mathcal{E}_{k+1}) = \mathbb{P}(\mathcal{E}_{k+1} \cap \mathcal{E}_k) = \mathbb{E}[\mathbb{E}[\mathbf{1}(\mathcal{E}_{k+1})|\mathcal{F}_k]\mathbf{1}(\mathcal{E}_k)] \geq (1 - \frac{\nu}{K})\mathbb{P}(\mathcal{E}_k). \quad (36)$$

As a result, we have, $\mathbb{P}(\mathcal{E}_K) \geq (1 - \frac{\nu}{K})^K \mathbb{P}(\mathcal{E}_0) > 1 - \nu$. Recall that

$$\theta^{(k+1)} = \theta^{(k)} - \eta \widehat{\nabla}_\theta C(\theta^{(k)}).$$

On the event \mathcal{E}_K and based on the smoothness of the function $C(\theta)$ established in Lemma C.2, we have

$$C(\theta^{(k+1)}) \leq C(\theta^{(k)}) + \underbrace{\langle \nabla_{\theta} C(\theta^{(k)}), \theta^{(k+1)} - \theta^{(k)} \rangle}_{e_1} + \underbrace{\frac{L_C}{2} \|\theta^{(k+1)} - \theta^{(k)}\|^2}_{e_2}$$

For e_1 , we have

$$\begin{aligned} e_1 &= \langle \nabla_{\theta} C(\theta^{(k)}), -\eta \widehat{\nabla}_{\theta} C(\theta^{(k)}) \rangle \\ &\leq -\eta \langle \nabla_{\theta} C(\theta^{(k)}), \widehat{\nabla}_{\theta} C(\theta^{(k)}) \rangle + \frac{\eta}{2} \|\nabla_{\theta} C(\theta^{(k)})\|^2 \\ &= -\eta \langle \nabla_{\theta} C(\theta^{(k)}), \widehat{\nabla}_{\theta} C(\theta^{(k)}) \rangle + \frac{\eta}{2} \|\nabla_{\theta} C(\theta^{(k)})\|^2 + \frac{\eta}{2} \|\widehat{\nabla}_{\theta} C(\theta^{(k)})\|^2 - \frac{\eta}{2} \|\widehat{\nabla}_{\theta} C(\theta^{(k)})\|^2 \\ &= \frac{\eta}{2} \|\widehat{\nabla}_{\theta} C(\theta^{(k)}) - \nabla_{\theta} C(\theta^{(k)})\|^2 - \frac{\eta}{2} \|\widehat{\nabla}_{\theta} C(\theta^{(k)})\|^2 \end{aligned}$$

For e_2 , we have

$$\begin{aligned} e_2 &= \frac{\eta^2 L_C}{2} \|\widehat{\nabla}_{\theta} C(\theta^{(k)})\|^2 \\ &\leq \frac{\eta^2 L_C}{2} \left(\|\widehat{\nabla}_{\theta} C(\theta^{(k)})\|^2 + \|\widehat{\nabla}_{\theta} C(\theta^{(k)}) - 2\nabla_{\theta} C(\theta^{(k)})\|^2 \right) \\ &= \frac{\eta^2 L_C}{2} \left(2\|\widehat{\nabla}_{\theta} C(\theta^{(k)})\|^2 + 4\|\nabla_{\theta} C(\theta^{(k)})\|^2 - 4\langle \widehat{\nabla}_{\theta} C(\theta^{(k)}), \nabla_{\theta} C(\theta^{(k)}) \rangle \right) \\ &= \frac{\eta^2 L_C}{2} \left(2\|\nabla_{\theta} C(\theta^{(k)})\|^2 + 2\|\widehat{\nabla}_{\theta} C(\theta^{(k)}) - \nabla_{\theta} C(\theta^{(k)})\|^2 \right). \end{aligned}$$

Then we have

$$\begin{aligned} C(\theta^{(k+1)}) &\leq C(\theta^{(k)}) + e_1 + e_2 \\ &\leq C(\theta^{(k)}) - \left(\frac{\eta}{2} - \eta^2 L_C\right) \|\nabla_{\theta} C(\theta^{(k)})\|^2 + \left(\frac{\eta}{2} + \eta^2 L_C\right) \|\widehat{\nabla}_{\theta} C(\theta^{(k)}) - \nabla_{\theta} C(\theta^{(k)})\|^2, \end{aligned} \quad (37)$$

which, combined with Lemma C.3, yields that with probability at least $1 - \nu$,

$$C(\theta^{(k+1)}) \leq C(\theta^{(k)}) - \left(\frac{\eta}{2} - \eta^2 L_C\right) \|\nabla_{\theta} C(\theta^{(k)})\|^2 + \left(\frac{\eta}{2} + \eta^2 L_C\right) e_{grad}. \quad (38)$$

Telescoping equation (38) over k from 0 to $K - 1$ yields

$$\frac{1}{K} \left(\frac{1}{2} - \eta L_C\right) \sum_{k=0}^{K-1} \|\nabla_{\theta} C(\theta^{(k)})\|^2 \leq \frac{C(\theta^{(0)}) - C(\theta^*)}{\eta K} + \left(\frac{1}{2} + \eta L_C\right) e_{grad}. \quad (39)$$

Substituting $\eta = \frac{1}{4L_C}$, $\epsilon = e_{grad}$ in equation (39) yields

$$\frac{1}{K} \sum_{k=0}^{K-1} \|\nabla_{\theta} C(\theta^{(k)})\|^2 \leq \frac{16L_C(C(\theta^{(0)}) - C(\theta^*))}{K} + 3\epsilon. \quad (40)$$

This leads to

$$\min_k \|\nabla_{\theta} C(\theta^{(k)})\|^2 \leq \frac{16L_C(C(\theta^{(0)}) - C(\theta^*))}{K} + 3\epsilon. \quad (41)$$

□

D. Experiment Details

We have released the DiffOP source codes and different simulation environments/systems in this paper as two standalone packages, both of which will be available at Github. In this section, we present the system setup, the implementation details of all approaches, and additional timing results for the simulation experiments.

D.1. System/Environment Setup

We note the environments are consistent to those considered in work (Jin et al., 2020). The dynamics of a two-link robot arm can be found in (Spong & Vidyasagar, 2008), page 171; and the dynamics of a quadrotor system can be found in (Jin et al., 2020), page 4. We include them here for completeness.

Cartpole control. The state vector is $x = [y, \phi, \dot{y}, \dot{\phi}]^T \in \mathbb{R}^4$ and the control input $u = F \in \mathbb{R}$ is the force. The dynamics is given by:

$$\frac{d}{dt} \begin{bmatrix} y \\ \phi \\ \dot{y} \\ \dot{\phi} \end{bmatrix} = \begin{bmatrix} \dot{y} \\ \dot{\phi} \\ \frac{F + m_p \sin(q)(l\dot{q}^2 + g \cos(q))}{m_c + m_p \sin^2(q)} \\ \frac{-F \cos(q) - m_p l \dot{q}^2 \sin(q) \cos(q) - (m_c + m_p)g \sin(q)}{l(m_c + m_p \sin^2(q))} \end{bmatrix},$$

where m_c is cart mass, m_p is pendulum mass, l is the length of the pole and g is the acceleration due to gravity. The control objective is defined as

$$c(x, u) = \|q(x - x_{\text{goal}})\|^2 + Ru^2,$$

where x_{goal} is the goal state, and $q \in \mathbb{R}^4$, $R \in \mathbb{R}$ are the cost parameters.

Two-link robot arm. The state vector is $x \in [q_1, q_2, \dot{q}_1, \dot{q}_2]^T \in \mathbb{R}^4$ with $q = [q_1, q_2]^T \in \mathbb{R}^2$ the vector of joint angles and $\dot{q} = [\dot{q}_1, \dot{q}_2]^T \in \mathbb{R}^2$ the vector of joint angular velocities, and the control input $u \in \mathbb{R}^2$ is the vector of torques applied to each joint. The dynamics of a two-link robot arm is given by:

$$\frac{d}{dt} \begin{bmatrix} q_1 \\ q_2 \\ \dot{q}_1 \\ \dot{q}_2 \end{bmatrix} = \begin{bmatrix} \dot{q}_1 \\ \dot{q}_2 \\ M(q)^{-1}(u - C(q, \dot{q})\dot{q} - G(q)) \end{bmatrix}$$

where $M(q) \in \mathbb{R}^{2 \times 2}$, $C(q, \dot{q}) \in \mathbb{R}^2$, $G(q) \in \mathbb{R}^2$ are the inertia matrix, Coriolis and centrifugal forces and gravity vector.

The control objective is defined as

$$c(x_t, u_t) = (x_t - x_{\text{goal}})^T Q (x_t - x_{\text{goal}}) + u^T R u.$$

where x_{goal} is the goal state and $Q \in \mathbb{R}^{4 \times 4}$, $R \in \mathbb{R}^{2 \times 2}$ are the cost parameters.

Quadrotor control. The state of the quadrotor system is $x \in [p, v, q, w]^T \in \mathbb{R}^{13}$. $p \in \mathbb{R}^3$ and $v \in \mathbb{R}^3$ are the position and velocity vector of the quadrotor; $q \in \mathbb{R}^4$ and $w = [w_x, w_y, w_x]^T \in \mathbb{R}^3$ are the unit quaternion and the angular velocity of the quadrotor. The control input $u = [T_1, T_2, T_3, T_4]^T \in \mathbb{R}^4$ is the thrusts of the four rotating propellers of the quadrotor. The dynamics of a quadrotor is given by:

$$\frac{d}{dt} \begin{bmatrix} p \\ v \\ q \\ w \end{bmatrix} = \begin{bmatrix} v \\ \frac{1}{m}(mg + f) \\ \frac{1}{2}\Omega(w)q \\ J^{-1}(M - w \times Jw) \end{bmatrix},$$

where m is the mass of the quadrotor, $J \in \mathbb{R}^{3 \times 3}$ is the moment of inertia of the quadrotor with respect to its body frame; $\Omega(w)$ is

$$\Omega(w) = \begin{bmatrix} 0 & -w_x & -w_y & -w_z \\ w_x & 0 & w_z & -w_y \\ w_y & -w_z & 0 & w_x \\ w_z & w_y & -w_x & 0 \end{bmatrix},$$

and used for quaternion multiplication. We denote the force vector applied to the quadrotor's center of mass (COM) to be $f \in \mathbb{R}^3$. The control input can effect the force magnitude $\|f\| \in \mathbb{R}$ and torque $M = [M_x, M_y, M_z]^T \in \mathbb{R}^3$:

$$\begin{bmatrix} \|f\| \\ M_x \\ M_y \\ M_z \end{bmatrix} = \begin{bmatrix} 1 & 1 & 1 & 1 \\ 0 & -l_w/2 & 0 & l_w/2 \\ -l_w/2 & 0 & l_w/2 & 0 \\ c & -c & c & -c \end{bmatrix} \begin{bmatrix} T_1 \\ T_2 \\ T_3 \\ T_4 \end{bmatrix},$$

with l_w being the wing length of the quadrotor and c a fixed constant.

The control objective is defined as

$$c(x, u) = \frac{\alpha_1}{2} \text{Tr}(I - R(q_g)^\top R(q)) + \alpha_2 \|p - p_g\|^2 + \alpha_3 \|v - v_g\|^2 + \alpha_4 \|w - w_g\|^2.$$

where q_g, p_g, v_g, w_g is the goal state, $R(q) \in \mathbb{R}^{3 \times 3}$ are the direction cosine matrix directly corresponding to q (See (Jin et al., 2020) for more details), $\alpha_1 \in \mathbb{R}, \alpha_2 \in \mathbb{R}, \alpha_3 \in \mathbb{R}, \alpha_4 \in \mathbb{R}$ are the cost coefficients.

Building control. The system state $x \in \mathbb{R}^1$ is zone temperature, control action $u \in \mathbb{R}^1$ is supply water temperature, and disturbance variables $d \in \mathbb{R}^7$ include outdoor air temperature, outdoor air relative humidity, diffuse solar radiation, direct solar radiation, occupancy flag, wind speed and wind direction. The simulation is modeled with EnergyPlus model (Crawley et al., 2001), original produced by (Zhang & Lam, 2018), and adapted by (Chen et al., 2019a). **Dynamics discretization.** The dynamical systems for nonlinear system control are discretized using the Euler method: $x_{t+1} = x_t + \Delta t \cdot f(x_t, u_t)$ with the discretization interval $\Delta t = 0.05\text{s}$ or $\Delta t = 0.1\text{s}$. For building control, $\Delta t = 5\text{minutes}$.

Simulation environment source codes. We have made different simulation environments/systems as a standalone Python package, which will be available at github.

D.2. Implementations for control policies.

Data acquisition. For *nonlinear control task*, we use a time horizon $T = 20$, consistent with the experimental setting in PDP control (Jin et al., 2020). We then collect a total of 20 trajectories from systems with random inputs $u_{1:T}$ drawn from a uniform distribution, using this data to train the dynamic model. For *building control*, there is a built-in controller in Energyplus model. Following work (Chen et al., 2019a), we collect the history data of 3 month, during which the heating system is governed by the built-in controller. We collect data to train the cost model and dynamic model for DiffOP, PDP-control and MPC-ICNN.

DiffOP. We present the architecture of DiffOP for all the control tasks as follows. We note that for all the input neural networks (ICNN), we utilize the softplus activation function to ensure the hessian is positive definite. We denote i as the planning step.

- Nonlinear control: The planning horizon is $H = 3$. The dynamic model is parameterized by an ICNN with a layer structure $n + m-4-n$. The cost is parameterized by a quadratic cost objective.
- Building control: The planning horizon is $H = 12$. The dynamic model is parameterized by a linear model $x_{i+1} = x_i + \Delta t \cdot \theta_f^\top [x_i^\top, u_i^\top, d_i^\top]^\top$, $\theta_f \in \mathbb{R}^{(n+m+p)n}$. The energy consumption is parameterized by an input convex neural network with a layer structure $(n + m)-12-1$.

For the policy gradient estimation in nonlinear control, we choose $N = 10$ as the number of trajectory samples. For building control, we consider each natural day as an iteration to update the policy parameters.

Pontryagin Differentiable Programming (PDP) control framework. We follow the methodology outlined (Jin et al., 2020) and utilize their published code to conduct our experiments. We assume the true cost model is *known*, and we model each system with a linear model $x_{i+1} = x_i + \Delta t \cdot \theta^\top [x_i^\top, u_i^\top]^\top$. Here the policy parameter of the PDP control is $\theta \in \mathbb{R}^{(m+n) \times n}$. At each iteration, we solve the control problem to obtain optimal control and predicted future state $u_{1:T}^*, x_{1:T}^*$, and then receive the true state $x_{1:T}$. We use the trajectory loss $\|x_{1:T} - x_{1:T}^*\|^2$ to update the dynamic model.

MPC-ICNN. For MPC-ICNN, we follow the work (Chen et al., 2019b), where the control policy is modeled with a convex optimization-based policy. The dynamics is modeled with an input convex neural network (Amos et al., 2017) with a layer structure $(n + m)-4-n$. At each iteration, we solve the optimization problem and apply the optimal control to the system.

PPO. We adopt stable-baselines3 (Raffin et al., 2021) to implement the baseline PPO. The policy uses a two-layer MLP with 256 units per hidden layer.

D.3. Additional timings for nonlinear control experiments

The comparison of running time of DiffOP/MPC-ICNN and PDP-control is listed in Table 3. All the experiments are conducted at CPU Intel(R) Core(TM) i7- 9750H CPU @ 2.60GHz. By leveraging the convexity of the control policy,

	DiffOP (adapted to MPC-ICNN)		PDP-control	
	Forward	Backward	Forward	Backward
Cartpole	0.004	0.002	0.02	0.03
RobotArm	0.005	0.004	0.02	0.03
Quadrotor	0.005	0.004	0.07	0.06

Table 3. Comparison for running time per time step for the optimization-based policies.

we compute the optimal policy through gradient descent methods implemented in PyTorch, while PDP control is solved using the CasADi optimization framework (Andersson et al., 2019). We note while the original MPC-ICNN (Chen et al., 2019b) was implemented in TensorFlow, we provide a PyTorch implementation that integrates with our DiffOP framework, maintaining the same algorithmic structure but without online policy updates during environment interactions.